Tableau 1. *Coordonnées atomiques, facteurs d'agitation thermiques isotropes équivalents et écarts-type*

$$B_{\text{éq}} = \tfrac{4}{3}\textstyle\sum_i\sum_j\beta_{ij}\mathbf{a}_i.\mathbf{a}_j.$$

	x	y	z	$B_{\text{éq}}$(Å^2)
Br(1)	0,15785 (6)	0,19363 (8)	0,1484 (1)	2,94 (2)
Br(2)	0,35154 (8)	0	0,5357 (1)	2,85 (2)
Mn	0,29879 (11)	0	0,2011 (2)	2,18 (3)
Mg	0	0	$\frac{1}{2}$	1,87 (8)
O(1)	0,4224 (5)	0,1534 (7)	0,2305 (8)	3,22 (13)
O(2)	0,2692 (8)	0	−0,0752 (10)	3,32 (19)
O(3)	0,1128 (7)	0,1439 (8)	0,5308 (12)	4,54 (20)
O(4)	0,0310 (8)	0	0,7564 (11)	4,26 (27)

Tableau 2. *Distances* (Å) *et angles* (°) *dans l'octaèdre* $Mg(H_2O)_6$

Mg	O(3^{i})	O(3)	O(3^{ii})	O(3^{iii})	O(4^{i})	O(4)
O(3^{i})	2,045 (9)	4,089 (15)	2,887 (12)	2,896 (13)	2,900 (15)	2,889 (11)
O(3)	180,0 (3)	2,045 (9)	2,896 (13)	2,887 (12)	2,889 (11)	2,900 (15)
O(3^{ii})	89,8 (4)	90,2 (3)	2,045 (9)	4,089 (15)	2,900 (15)	2,889 (11)
O(3^{iii})	90,2 (4)	89,8 (4)	180,0 (4)	2,045 (9)	2,889 (11)	2,900 (15)
O(4^{i})	90,2 (4)	89,7 (4)	90,2 (4)	89,8 (4)	2,049 (9)	4,098 (15)
O(4)	89,8 (4)	90,2 (4)	89,8 (4)	90,2 (4)	180,0 (4)	2,049 (9)

Code de symétrie: (i) $-x, -y, 1-z$; (ii) $-x, y, 1-z$; (iii) $x, -y, z$; (iv) $\frac{1}{2}-x, \frac{1}{2}-y, -z$; (v) $1-x, y, 1-z$; (vi) $\frac{1}{2}-x, y-\frac{1}{2}, -z$; (vii) $\frac{1}{2}-x, \frac{1}{2}-y, 1-z$; (viii) $x, y, 1-z$; (ix) $x, y, 1+z$.

Tableau 3. *Distances* (Å) *et angles* (°) *dans le polyèdre* $MnBr_3(H_2O)_3$ (*code de symétrie: voir Tableau* 2)

Mn	Br(1)	Br(1^{iii})	Br(2)	O(1)	O(1^{iii})	O(2)
Br(1)	2,641 (2)	3,884 (3)	3,892 (3)	3,404 (7)	4,852 (8)	3,405 (10)
Br(1^{iii})	94,69 (10)	2,641 (2)	3,892 (3)	4,852 (8)	3,404 (7)	3,405 (10)
Br(2)	94,70 (6)	94,70 (6)	2,651 (2)	3,414 (8)	3,414 (8)	4,863 (10)
O(1)	88,6 (2)	175,1 (3)	88,6 (2)	2,215 (7)	3,077 (10)	3,076 (9)
O(1^{iii})	175,1 (2)	88,6 (2)	88,6 (2)	88,0 (3)	2,215 (7)	3,076 (9)
O(2)	88,6 (2)	88,6 (2)	175,2 (3)	87,9 (3)	87,9 (3)	2,217 (9)

Tableau 4. *Liaisons hydrogène prévues* (*code de symétrie: voir Tableau* 2)

O(1)$\cdots$Br(1^{iv})	3,354 (7)	O(3)$\cdots$Br(1)	3,522 (11)
O(1)$\cdots$Br(2^{v})	3,352 (7)	O(3)$\cdots$Br(2)	3,513 (10)
O(2)$\cdots$Br(1^{iv})	3,351 (5)	O(4)$\cdots$O(2^{ix})	3,009 (15)
O(2)$\cdots$Br(1^{vi})	3,351 (5)	O(4)$\cdots$Br(1^{i})	3,515 (10)
O(3)$\cdots$O(1^{vii})	3,015 (12)	O(4)$\cdots$Br(1^{ii})	3,515 (10)

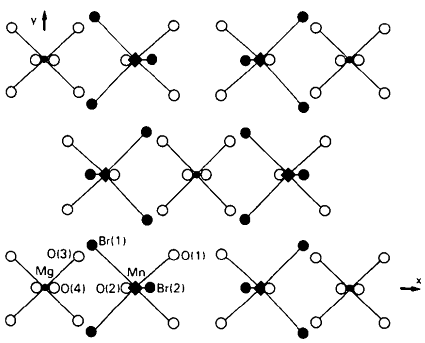

Fig. 1. Projection de la structure suivant **c**.

M—Br ≃ 2,76 Å supérieures à celles observées dans cette structure (Mn—Br = 2,641 Å).

Ces polyèdres $Mg(H_2O)_6$ et $MnBr_3(H_2O)_3$ se répartissent dans des couches stoechiométriques perpendiculaires à l'axe b (Fig. 1). La cohésion de l'édifice cristallin est assurée par des liaisons hydrogènes entre les polyèdres de coordination (Tableau 4). Les distances permettent de prévoir que chaque molécule d'eau liée au magnésium échange une liaison simple avec une molécule d'eau du polyèdre de coordination du manganèse, et une liaison bifurquée sur deux ions brome alors que les molécules d'eau liées au manganèse n'échangent que des liaisons hydrogène simples avec des ions brome.

Références

Balarev, C. & Duhlev, R. (1983). *Zh. Neorg. Khim.* **28**, 2639–2646.

Coppens, P. & Hamilton, W. C. (1970). *Acta Cryst.* A**26**, 71–83.

International Tables for X-ray Crystallography (1974). Tome IV. Birmingham: Kynoch Press.

Meulenaer, J. de & Tompa, H. (1965). *Acta Cryst.* **19**, 1014–1018.

Acta Cryst. (1985). C**41**, 170–173

Tribarium Titanium(IV) Diruthenate(IV), $Ba_3TiRu_2O_9$, a Rietveld Refinement of Neutron Powder Diffraction Data

By D. Verdoes, H. W. Zandbergen and D. J. W. IJdo

Gorlaeus Laboratories, State University, Leiden, PO Box 9502, 2300 *RA Leiden, The Netherlands*

(*Received* 16 *May* 1984; *accepted* 27 *September* 1984)

Abstract. $M_r = 806{\cdot}11$, hexagonal, $Z = 2$, $P6_3/mmc$. At room temperature: $a = 5{\cdot}7155$ (1), $c = 14{\cdot}0298$ (5) Å, $V = 396{\cdot}92$ (2) Å^3, $D_x = 6{\cdot}7450$ (4) Mg m^{-3}. At 1·2 K: $a = 5{\cdot}7046$ (1), $c = 14{\cdot}0080$ (6) Å, $V = 394{\cdot}78$ (2) Å^3, $D_x = 6{\cdot}7815$ (4) Mg m^{-3}. The structure has been refined by Rietveld analysis of powder neutron diffraction data recorded at room temperature and at 1·2 K [$\lambda =$

0108-2701/85/020170-04$01.50

2·5904 (5) Å, R_I = 1·71, 2·44, R_P = 6·63, 7·30, R_{wP} = 7·26, 7·40%, respectively, both for 53 reflections]. The structure at both temperatures is of a hexagonal, 6*L* type. BaO_3 layers are stacked $(hcc)_2$, resulting in strings of two face-sharing octahedra, which share corners with single octahedra.

Introduction. In a research program to investigate compounds with perovskite or related structures on their properties as a host lattice for nuclear waste, we investigated the system $BaTiO_3$–$BaRuO_3$. It was found that a 6*L* structure occurred with a phase width depending on the firing temperature. $Ba_3TiRu_2O_9$ was prepared, assuming that Ti would occupy the corner-sharing octahedra and Ru the face-sharing ones. $Ba_3Ti_2RuO_9$ and $Ba_4Ti_3RuO_{12}$ (Dickson, Katz & Ward, 1959) were reported to have the hexagonal $BaTiO_3$ structure. The magnetic data of $Ba_3Ti_2RuO_9$ were reported in an article about compounds with the hexagonal barium titanate structure (Dickson, Katz & Ward, 1961).

Experimental. AR starting materials $BaCO_3$, TiO_2 and Ru thoroughly mixed in an agate mortar in the appropriate ratios. The mixtures $BaTi_xRu_{1-x}O_3$ (x = 0·25, 0·50, 0·75) heated in an Al_2O_3 crucible at 1073 K for 1 d and at 1273 K for 3 d, both in air, and at 1473 K in a Pt capsule for 1 week. X-ray powder diffraction patterns obtained, after firing at 1273 and 1473 K, with a Philips PW 1050 diffractometer. After firing at 1273 K $BaTi_xRu_{1-x}O_3$ for $x = 0{\cdot}50$ contained only 6*L*-type reflections; for $x = 0{\cdot}25$ and 0·75 in addition to the 6*L*-type reflections were also found reflections of $BaRuO_3$ and $BaTiO_3$ respectively. After firing at 1473 K only 6*L*-type reflections observed for all three samples.

All lines could be indexed with a hexagonal unit cell, with absent reflections hhl, $l = 2n + 1$. Since no single crystals were available Rietveld's (1969) method for refinement of neutron powder diffraction data for the composition $Ba_3TiRu_2O_9$ was used, with the assumption that Ti would occupy the corner-sharing octahedra and Ru the face-sharing ones. Data in the range $5° < 2\theta < 163°$ in steps of 0·1°; neutrons of wavelength 2·5904 (5) Å at 300 and 1·2 K from the (111) planes of a Cu crystal; pyrolytic graphite with a total thickness of 120 mm as a second-order filter; Soller slits, horizontal divergence 30′, placed between the reactor and the monochromator and in front of each of the four ^3He counters; sample holder (∅ = 20 mm) consisted of a V tube, closed with Cu plugs fitted with O-rings. No precautions against preferred orientations. Maximum absorption correction 3%, $\mu R = 0{\cdot}34$ (Weber, 1967). Background determined from parts in the diagram which did not contain any contribution from reflections, and extrapolation between these points. Statistically expected values of R_{wP} 3·99 and 3·62% for, respectively, 1·2 and 300 K.

The hexagonal $BaTiO_3$ structure (space group $P6_3/mmc$, Burbank & Evans, 1948) was used as a trial model: Ba(1) in 2(*b*) $(0,0,\frac{1}{4})$, Ba(2) in 4(*f*) $(\frac{1}{3},\frac{2}{3},z)$, Ti(1) in 2(*a*) (0,0,0), Ti(2) in 4(*f*), Ru(1) in 4(*f*), Ru(2) in 2(*a*), O(1) in 6(*h*) $(x,2x,\frac{1}{4})$, O(2) in 12(*k*) $(x,2x,z)$. 20 parameters in the refinement: a scale factor, three half-width parameters defining the Gaussian line shape of the reflections, the counter zero error, a preferred-orientation parameter, an asymmetry parameter below $2\theta = 37°$, the unit-cell parameters, the atomic positional parameters, the isotropic thermal parameters and the occupation rates of Ti and Ru. The coherent scattering lengths used are: Ba 5·25, Ti −3·44, Ru 7·21, O 5·805 fm (Koester, Rauch, Herkens & Schroeder, 1981). The Rietveld program minimizes the function $X^2 = \sum_i w_i[y_i(\text{obs.}) - (1/c)y_i(\text{calc.})]^2$, where y_i(obs.) and y_i(calc.) are the observed and calculated data points, w_i is the statistical weight $[1/y_i(\text{obs.})]$ allotted to each data point and c is the scale factor. The following R factors were calculated:

$$R_I = 100\sum|I_i(\text{obs.}) - (1/c)I_i(\text{calc.})|/\sum I_i(\text{obs.});$$

$$R_P = 100\sum|y_i(\text{obs.}) - (1/c)y_i(\text{calc.})|/\sum y_i(\text{obs.});$$

$$R_{wP} = 100[\sum w_i|y_i(\text{obs.}) - (1/c)y_i(\text{calc.})|^2/\sum w_i|y_i(\text{obs.})|^2]^{1/2};$$

where I_i(obs.) and I_i(calc.) are the observed and calculated integrated intensities of each reflection. During the last cycle Δ/σ was smaller than 0·03.

Refinements carried out in space groups with the same systematically absent reflections did not lead to significantly smaller R values. The stability in water at 573 K and 0·2 GPa was tested for 1 d; the compound was stable under these conditions. Earlier we found (Zandbergen & IJdo, 1984) that perovskite-like compounds with Ru^{5+} decompose completely under these conditions.

The agreement between the observed* and calculated profiles is shown in Fig. 1.

Discussion. Atomic parameters are given in Table 1, distances and angles in Table 2. The structure of $Ba_3TiRu_2O_9$ is shown in Fig. 2. The structure is a substituted 6*L* hexagonal $BaTiO_3$ structure (Burbank & Evans, 1948), in which the BaO_3 layers are stacked $(hcc)_2$. There is a sequence along the c axis of a single octahedron which shares corners with pairs of face-shared octahedra.

This structure was not unexpected because it is an intermediate structure between the 3*L* and 9*L* structures.

---

* The numerical intensity of each measured point, as a function of the angle, and some additional experimental details have been deposited with the British Library Lending Division as Supplementary Publication No. SUP 39746 (13 pp.). Copies may be obtained through The Executive Secretary, International Union of Crystallography, 5 Abbey Square, Chester CH1 2HU, England.

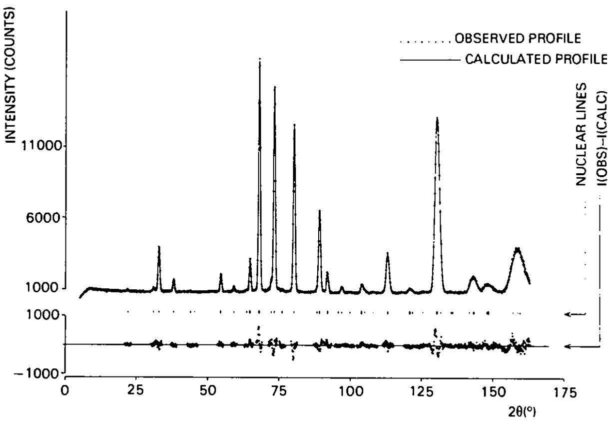

Fig. 1. The observed and calculated profile of $Ba_3TiRu_2O_9$ at 300 K.

Table 1. *Fractional atomic coordinates, occupation rates and thermal parameters*

$Ba_3TiRu_2O_9$ at 300 K

	x	*z*	*n*	*B*(Å^2)
Ba(1)	0	0·25	0·16667	1·7 (2)
Ba(2)	0·33333	0·0913 (4)	0·33333	1·1 (1)
Ti(1)	0	0	0·093 (1)	0·6 (1)
Ti(2)	0·33333	0·8399 (3)	0·074 (1)	0·6 (1)
Ru(1)	0·33333	0·8399 (3)	0·259 (1)	0·6 (1)
Ru(2)	0	0	0·074 (1)	0·6 (1)
O(1)	0·5115 (3)	0·25	0·5	0·8 (1)
O(2)	0·8350 (3)	0·0802 (1)	1·0	1·1 (1)

$Ba_3TiRu_2O_9$ at 1·2 K

	x	*z*	*n*	*B*(Å^2)
Ba(1)	0	0·25	0·16667	1·3 (2)
Ba(2)	0·33333	0·0909 (5)	0·33333	0·5 (1)
Ti(1)	0	0	0·095 (1)	0·3 (1)
Ti(2)	0·33333	0·8393 (3)	0·072 (1)	0·3 (1)
Ru(1)	0·33333	0·8393 (3)	0·262 (1)	0·3 (1)
Ru(2)	0	0	0·072 (1)	0·3 (1)
O(1)	0·5111 (4)	0·25	0·5	0·4 (1)
O(2)	0·8363 (4)	0·0804 (1)	1·0	0·8 (1)

Table 2. *Atomic distances* (Å) *and angles* (°) *in* $Ba_3TiRu_2O_9$

a (about) equilateral distances.

	300 K	1·2 K
Ba(1)—O(1)*a*	2·860 (3)	2·854 (3)
Ba(1)—O(2)	2·890 (2)	2·885 (3)
Ba(2)—O(1)	2·839 (5)	2·847 (6)
Ba(2)—O(2)*a*	2·862 (3)	2·856 (3)
Ba(2)—O(2)	2·928 (6)	2·936 (7)
[Ti(1),Ru(2)]—O_6 octahedron		
Ti(1)—O(2)	1·982 (3)	1·974 (3)
O(2)—O(2)*a*	2·829 (4)	2·801 (9)
O(2)—O(2)	2·777 (4)	2·782 (6)
O(2)—Ti(1)—O(2)	91·1 (1)	90·4 (1)
[Ru(1),Ti(2)]$_2$O$_9$ group		
Ru(1)—O(1)	1·984 (4)	1·986 (4)
Ru(1)—O(2)	2·012 (4)	2·022 (4)
Ru(1)—Ru(1)	2·515 (6)	2·515 (7)
O(1)—O(1)*a*	2·658 (9)	2·662 (9)
O(1)—O(2)	2·874 (3)	2·881 (4)
O(2)—O(2)*a*	2·887 (4)	2·903 (5)
O(1)—Ru(1)—O(1)	84·1 (2)	84·2 (2)
O(1)—Ru(1)—O(2)	174·7 (2)	174·7 (2)
O(1)—Ru(1)—O(2)	92·0 (1)	91·9 (1)

Above 393 K and normal pressure $BaTiO_3$ is a 3*L* structure (*c*) [Wyckoff (1964), see Fig. 3], whereas at high temperature a 6*L* structure occurs, $(hcc)_2$. This transition results in an increase in the volume of 4% (Burbank & Evans, 1948).

At room temperature and normal pressure $BaRuO_3$ is a 9*L* structure, $(hhc)_3$ [Donohue, Katz & Ward (1965), see Fig. 4], and transforms at first to a 4*L* structure, $(hc)_2$, and at higher pressure to a 6*L* structure, $(hcc)_2$. The transition from a 9*L* to a 6*L* structure results in a decrease in the volume of 5% (Longo & Kafalas, 1968).

In the 9*L* $BaRuO_3$ structure Ru is situated in face-shared octahedra, while Ti in 3*L*-$BaTiO_3$ occupies the single octahedra. Because of this it was expected that in $Ba_3TiRu_2O_9$ Ti would occupy the single octahedra and Ru the faced-shared octahedra. It was found that Ti occupies 57% of the single octahedra, while in the case of a random distribution there would be an occupation rate of 33%. This shows that Ti still has a preference for the single octahedra, while Ru still prefers the face-shared octahedra. The occurrence of Ti

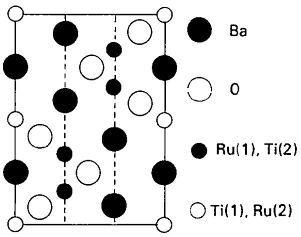

Fig. 2. The (110) plane of 6*L*-$Ba_3TiRu_2O_9$.

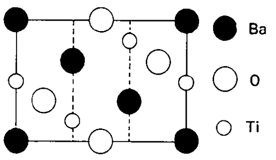

Fig. 3. The (110) plane of 3*L*-$BaTiO_3$.

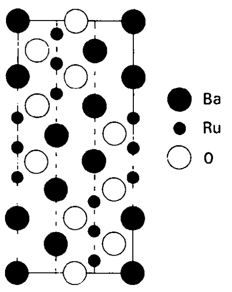

Fig. 4. The (110) plane of 9*L*-$BaRuO_3$.

as well as Ru at both positions can be understood, since the ions have almost the same radii, 0·605 and 0·620 Å respectively (Shannon, 1976), and both $BaTiO_3$ and $BaRuO_3$ occur with the $6L$ structure.

The distance between the metal atoms in the $[Ru(1),Ti(2)]_2O_9$ group is too short to form regular face-shared octahedra. Because of the repulsion between the metal atoms, they are not exactly at the centers of the face-sharing octahedra. This results in a shorter O(1)—O(1) distance in the common face and in the angle O(1)—metal—O(2) being larger than 90°.

The metal—metal distance is very short (2·515 Å), suggesting intermetallic bonding. This intermetallic bond is also reported in the $9L$-$BaRuO_3$ structure, in which the Ru—Ru distance is 2·55 Å (Donohue, Katz & Ward, 1965).

In $Ba_3SrNb_2O_9$ (Zandbergen & IJdo, 1983) the Nb—Nb distance is 2·97 Å, while in $Ba_3SrRu_2O_9$ (Zandbergen & IJdo, 1984) the Ru—Ru distance is 2·67 Å. This difference is due to the atomic radius of Nb^{5+}, which is larger than that of Ru^{5+}, 0·64 Å and 0·565 Å respectively (Shannon, 1976). The difference in Ru—Ru distance in $Ba_3TiRu_2O_9$ and $Ba_3SrRu_2O_9$ is probably the result of the difference in valence of the Ru atoms, which is respectively 4+ and 5+.

In an undeformed packing with ideal octahedra the axial ratio $c/a = \sqrt{6} = 2{\cdot}449$ (Zandbergen & IJdo, 1983). For $Ba_3TiRu_2O_9$ the axial ratios are 2·455 at 300 K and 2·456 at 1·2 K. A tilt around the threefold axes decreases the lattice parameter a and thus increases c/a. Because the c/a values are close to the expected value, we expect that the tilt is zero.

This research project was partly financed by the Commission of the European Communities. The authors are indebted to Mr J. F. Strang of Energieonderzoek Centrum Nederland, Petten, for collection of the neutron diffraction data.

References

BURBANK, R. D. & EVANS, H. T. (1948). *Acta Cryst.* **1**, 330–336.

DICKSON, J. G., KATZ, L. & WARD, R. (1959). *J. Am. Chem. Soc.* **81**, 4109.

DICKSON, J. G., KATZ, L. & WARD, R. (1961). *J. Am. Chem. Soc.* **83**, 3026–3029.

DONOHUE, P. C., KATZ, L. & WARD, R. (1965). *Inorg. Chem.* **4**, 687–692.

KOESTER, L., RAUCH, H., HERKENS, M. & SCHROEDER, K. (1981). Kernforschungsanlage Rep., Jülich, p. 1755.

LONGO, J. M. & KAFALAS, J. A. (1968). *Mater. Res. Bull.* **3**, 687–692.

RIETVELD, H. M. (1969). *J. Appl. Cryst.* **2**, 65–71.

SHANNON, R. D. (1976). *Acta Cryst.* A**32**, 751–767.

WEBER, K. (1967). *Acta Cryst.* **23**, 720–725.

WYCKOFF, R. W. G. (1964). *Crystal Structures*, Vol. 2. New York: Interscience.

ZANDBERGEN, H. W. & IJDO, D. J. W. (1983). *Acta Cryst.* C**39**, 829–832.

ZANDBERGEN, H. W. & IJDO, D. J. W. (1984). *Acta Cryst.* C**40**, 919–922.

Acta Cryst. (1985). C**41**, 173–177

Structure of the Intermediate Phase, $Li_{2.09}W_{0.91}Nb_{0.09}O_4$, in the Li_2WO_4–Li_3NbO_4 System

BY RENU SHARMA AND MONICA LUNDBERG

Department of Inorganic Chemistry, Arrhenius Laboratory, University of Stockholm, S-106 91 Stockholm, Sweden

(*Received* 2 *May* 1984; *accepted* 1 *October* 1984)

Abstract. $M_r = 254{\cdot}2$, triclinic, $P\bar{1}$, $a = 7{\cdot}967\,(2)$, $b = 7{\cdot}774\,(1)$, $c = 5{\cdot}271\,(1)$ Å, $\alpha = 90{\cdot}61\,(2)$, $\beta = 103{\cdot}41\,(2)$, $\gamma = 105{\cdot}81\,(2)$°, $V = 304{\cdot}6\,(1)$ Å^3, $Z = 4$, $D_m = 5{\cdot}518$, $D_x = 5{\cdot}543\,(2)$ g cm^{-3}, λ(Mo $K\alpha$) = 0·71069 Å, $\mu = 367$ cm^{-1}, $F(000) = 437$, $T = 293$ K, final $R = 0{\cdot}047$ for 2125 observed reflections. The O atoms are in approximate cubic close-packing with (W,Nb) atoms in octahedral interstices, arranged so that $(W,Nb)_4O_{16}$ groups are created. These groups are connected through a three-dimensional framework of edge-sharing LiO_6 octahedra and Li_4O_{10} groups of edge-sharing LiO_4 tetrahedra.

Introduction. The niobium–tungsten oxides containing alkali metals are of considerable interest as solid-state ionic conductors. Li^+ ions especially have been shown to be mobile in a voltage gradient, and therefore the Li–W–Nb–O system has been investigated at this laboratory (Hörlin, Marinder & Nygren, 1982).

The subsystem Li_2WO_4–Li_3NbO_4 was searched for non-stoichiometric compounds with partially occupied lithium sites. The phase analysis revealed one intermediate compound, which could be prepared as a single phase, with the composition $Li_{2.09}W_{0.91}Nb_{0.09}O_4$. This article will describe the results of the single-crystal

0108-2701/85/020173-05$01.50